Mol Biol Rep (2013) 40:3523–3535
DOI 10.1007/s11033-012-2426-x

The *OitaAG* and *OitaSTK* genes of the orchid *Orchis italica*: a comparative analysis with other C- and D-class MADS-box genes

Marinella Salemme · Maria Sica · Luciano Gaudio · Serena Aceto

Received: 13 September 2012 / Accepted: 18 December 2012 / Published online: 1 January 2013

Abstract According to the ABCDE model of flower development, the C- and D- class MADS box genes are involved in the formation of male and female reproductive organs (fused to form the column in orchids) and in ovule maturation (triggered by fertilization in orchids). In the present study, we report the isolation of the *Orchis italica* genes *OitaAG* and *OitaSTK*, homologs of the C-class *AGAMOUS* and the D-class *SEEDSTICK* genes of *Arabidopsis*, respectively. Analysis of their expression profiles reveals high levels of mRNA in columns and ovaries, particularly after pollination. However, weak expression is also detectable in the inner tepals (*OitaAG*) and the lip and root (*OitaSTK*). This expression profile is only partially overlapping with those reported in other orchid species and may be the consequence of a different evolutionary history of these functional gene classes in orchids. The genomic characterization of the *OitaAG* and *OitaSTK* genes shows that a high number of traces of mobile elements are present in introns and could have contributed to the size expansion of some of them (e.g., intron 2 and 3 of *OitaAG* and intron 3, 4 and 5 of *OitaSTK*). Nucleotide sequences of intron 1 of the *OitaSTK* gene and other *STK*-like genes do not share regulatory motifs, whereas sequence comparison of intron 2 of the *OitaAG* gene with that of intron 2 of other *AG*-like genes reveals, for the first time in an orchid species, the presence of conserved *cis*-regulatory boxes and binding sites for transcription factors that positively (e.g., LEAFY and WUSCHEL) or negatively (e.g., BELLRINGER) regulate the expression of the *AG* homologs in dicots and monocots.

Keywords MADS-box · Orchidaceae · *cis*-Regulatory elements · Introns

Introduction

The family Orchidaceae is one of the largest among the flowering plants. It is characterized by great morphological diversification and specialization of the floral structures. The typical orchid flower shows bilateral symmetry and is composed of three sepals (termed outer tepals) and three petals divided into two lateral inner tepals and a lip (or labellum), a highly modified median inner tepal. The male and female reproductive organs are highly modified; they are fused and constitute a single structure known as column or gynostemium. The mature pollen grains (pollinia) are positioned at the top of the column. At the column base is the ovary, the development of which is triggered by fertilization [1–3].

The complex regulatory network that establishes flower development is well described by the ABCDE model, which integrates the role of the floral homeotic genes in a spatial and functional view [4, 5]. All but one (*APETALA2–AP2*) of the genes involved in the ABCDE model are MADS-box genes corresponding to various functional classes. Based on the latest version of the model (A)BCDE, the expression of B—(*PISTILLATA*/*GLOBOSA*-like and *APETALA3*/*DEFICIENS*-like) and C-class (*AGAMOUS*-like) genes alone regulates the formation of petals and carpels, respectively, while both classes drive the development of stamens. The A-class genes (*AP1*- and *AP2*-like) act at various different levels,

Electronic supplementary material The online version of this article (doi:10.1007/s11033-012-2426-x) contains supplementary material, which is available to authorized users.

M. Salemme · M. Sica · L. Gaudio · S. Aceto (✉)
Department of Biological Sciences, University of Naples Federico II, via Mezzocannone 8, 80134 Naples, Italy
e-mail: serena.aceto@unina.it

from floral meristem identity to the activation and definition of the expression domains of the B- and C-class genes [6]. The development of ovules is regulated mainly by the D--class genes (*SEEDSTICK*-like), and the formation of all floral structures is ensured by the action of the E-class genes (*SEPALLATA*-like). In brief, A- and E-class genes specify the formation of sepals; A-, B- and E-class genes drive the formation of petals; B-, C- and E-class genes determine the formation of stamens; C- and E-class genes specify the formation of carpels; D- and E-class genes are involved in the formation of ovules. Although the (A)BCDE model is applicable to a wide number of species [6–11], differences are emerging in the mechanisms leading to flower development in non-model species such as orchids [12]. For example, extensive analyses of the orchid B-class genes revealed their peculiar role in the formation of the orchid perianth [13] and the occurrence of lineage-specific duplication events [14–20].

In orchids, a number of C- and D-class genes have been identified. All are involved in various aspects of flower and ovule development, with some differences among the examined species, all belonging to the subfamily Epidendroideae [21–25]. In some species, e.g., *Phalaenopsis* and *Oncidium*, C- and D- class genes have redundant functions [21, 22, 25]; in others, e.g., *Dendrobium thyrsiflorum*, some differences in the expression profile are related to specific involvement in early or late ovule development [23]. In addition, in *Cymbidium ensifolium* a C-class duplication event followed by sub-functionalization gave rise to two functional paralogs [24].

The C- and D-class genes are sister clades, generated by a duplication event occurred early during angiosperm evolution [26]. All of the C- and D-class gene products share two motifs at the C-terminus: the AG motifs I and II [26]. In the model plant *Arabidopsis*, the expression of the C-class gene *AGAMOUS* (*AG*) is regulated by *cis*-acting elements present within the 3-kb intron 2 [27–29]. Some of these elements, such as the binding site of the direct activator LEAFY (LFY), are conserved among a wide number of species and are thought to pre-date the divergence between monocots and dicots [30]. Also the expression of the D-class gene *SEEDSTICK* (*STK*) of *Arabidopsis* seems to be regulated by multiple *cis*-acting elements located within the promoter region and the 1.3-kb intron 1. These regulatory motifs are GA-rich elements able to bind the BASIC PENTACYSTEINE 1 (BPC1) protein, with consequent DNA conformational changes [31].

In this study, we report the isolation, genomic characterization and expression of two genes in the orchid *Orchis italica* (subfamily Orchidoideae), *OitaAG* and *OitaSTK*. The genes *OitaAG* and *OitaSTK* belong to the MADS-box C- and D-class, respectively. In addition, we report for the first time in an orchid species the comparative analyses of intron 2 of the gene *OitaAG* and of intron 1 of the gene *OitaSTK* and their evolutionary implications.

Materials and methods

Isolation of *OitaAG* and *OitaSTK* cDNAs

Total RNA extraction from inflorescence of *O. italica* and cDNA synthesis were performed as previously described [15], using a MADS-box degenerate primer (5′-AAGATAGAGAATCCDACDAACD-3′) and a poly-T primer. After cDNA cloning, forty clones were screened by nucleotide sequencing on a 310 Automated Sequencer (Applied Biosystems). BLAST analysis revealed the presence in *O. italica* of two cDNAs named *OitaAG* and *OitaSTK*, which showed nucleotide similarity to C- and D-class MADS-box genes, respectively. To obtain the nucleotide sequence of the 5′-untranslated region (UTR), three specific reverse primers were designed for each cDNA (Table S1, supplementary material) and 5′ RACE experiments were performed using the 5′ RACE System (Invitrogen). The amplification products were cloned into pGEM-T Easy vector (Promega) and sequenced using the universal primers T7 and SP6. The nucleotide sequences of the *OitaAG* and *OitaSTK* cDNAs were deposited in GenBank with the accession numbers JX205496 and JX205497, respectively.

Expression analysis

Florets from early (10 days before anthesis, ~9 mm diameter size) and late (after anthesis) inflorescence of *O. italica* were dissected to collect the outer and inner tepal, lip, column and unpollinated ovary tissue. Both stages refer to a fully developed flower, with all floral organs formed. Thus, the two stages only differ in cell size. Compared to the fully opened flowers (late stage), in the bud stage (early stage) cell division is completed but cell distension is still occurring. Manual fertilization of ten ovaries was performed, and ovary tissue was collected 3, 7 and 10 days after pollination (dap). Ovary development of *O. italica* is shorter than that described in other orchids such as *Phalaenopsis* (~64 dap) [25]. In flowers of *O. italica* at the anthesis, the ovules are immature and contain the megaspore mother cell undergoing the first meiotic division. At 3 days after pollination the ovules are mature and the female gametophyte is fully developed; at 7 days after pollination, fecundation is already occurred and the seeds are in early development stages; at 10 days after pollination the seeds are almost mature with seed coats completely developed (Barone Lumaga, manuscript in preparation). In addition, leaf, stem and root tissue were collected. All of the dissected tissues were quickly stored in

RNA Later (Ambion) at −20 °C until total RNA extraction (TRIzol reagent, Ambion). After treatment with DNase I (Ambion), total RNA was quantified using the spectrophotometer Nanodrop 2000c (ThermoScientific). RNA integrity was checked by agarose gel electrophoresis.

Reverse transcription reactions were conducted using 350 ng of total RNA isolated from the different tissues with the Advantage RT PCR kit (Clontech) and oligo dT primers. Primer pairs that specifically amplified fragments of the *OitaAG*, *OitaSTK* and actin (*OitaAct*, GenBank accession number AB630020) cDNAs were designed using the software Primer Express v.3.0 (Applied Biosystems). Primer sequences are listed in Table S1 of the supplementary material.

Real time PCR was performed using a 7500 Real-Time PCR System (Applied Biosystems); cDNA (30 ng) from each tissue was used as previously described [16]. For all of the genes examined, the reactions were conducted in technical triplicates on two independent biological samples. Negative controls were performed without cDNA. For each well, the evaluation of PCR efficiency and optimal threshold cycle (C_T) of the target genes (*OitaAG* and *OitaSTK*) and the endogenous control gene (*OitaAct*) were performed using the REAL TIME PCR MINER online tool [32]. The mean relative expression ratio (rER) of the *OitaAG* and *OitaSTK* genes in the different tissues was calculated (with standard deviation) using *OitaAct* as the endogenous control gene and leaf cDNA as the reference sample [33]. Differences in the relative expression levels of the *OitaAG* and *OitaSTK* genes between and/or among different samples were assessed by the two-tailed *t* test and ANOVA followed by the Tukey HSD post hoc test, respectively.

PCR amplification of genomic DNA

Genomic DNA of *O. italica* was extracted from leaves using a modified Doyle & Doyle method [34]. Based on the nucleotide sequence of the *OitaAG* and *OitaSTK* cDNAs, several PCR primer pairs were designed to amplify the genomic region spanning from 5′- to 3′-UTR (Table S2, supplementary material). Most PCR amplifications were conducted using the LongAmp Taq PCR kit (New England Biolabs) using conditions previously described [35]. To amplify the genomic regions including intron 2 and intron 3 of the *OitaAG* locus and intron 2 and intron 5 of the *OitaSTK* locus, reactions were performed with two amplification rounds. The first round followed conditions previously described [36]. The second amplification was conducted using 1 µl of the first reaction and nested primers, with denaturation and annealing time and temperature suggested by the *Taq* manufacturer (New England Biolabs) and extension times ranging from 7 to 10 min at 65 °C for a total of 35 cycles. Amplification fragments of small size were cloned into the pGEM-T Easy vector, whereas large fragments were cloned using the CopyControl cDNA, Gene and PCR Cloning kit (Epicentre). Sequencing reactions were conducted using the pGEM-T Easy or pCC1 plasmid primers. For the large cloned amplicons, additional specific nested primers were progressively designed and used to sequence the complete fragments.

Sequence analysis

The nucleotide sequences of the *OitaAG* and *OitaSTK* cDNAs were virtually translated and aligned with those of AG-like and STK-like sequences of monocots retrieved from public databases (Table 1) using the MUSCLE software [37]. To avoid possible problems in the resolution of the phylogenetic tree due to high cytosine content in the nucleotide sequences encoding the C-terminus of these proteins in grasses (rice and maize), only the MADS, I and K domains were considered for the phylogenetic tree reconstruction [38]. The search for the best amino acid evolutionary model and the construction of the Maximum Likelihood (ML) tree were performed using MEGA5 software [39]. DAL2 of *Picea abies* was used as the outgroup. Bootstrap analysis on the ML tree was conducted with 1,000 replicates.

ontig assembly of *OitaAG* and *OitaSTK* genomic DNA sequences and alignment between cDNA and genomic DNA sequences was performed using BIOEDIT [40]. The accession numbers of the genomic sequences of the *OitaAG* and *OitaSTK* loci are JX205498 and JX205499 respectively.

Intron sequences from both the *OitaAG* and *OitaSTK* genes were screened for the presence of repetitive elements and traces of plant mobile elements using the CENSOR online tool [41] and BLAST analysis. CENSOR is a program that performs BLAST searches using REPBASE, a reference database of eukaryotic repetitive/mobile DNA, and provides a description of the repetitive/mobile elements found. The analysis was conducted using the default settings, selecting the Viridiplantae section of REPBASE.

Sequences of intron 2 of the *OitaAG* gene, of intron 1 of the *OitaSTK* gene and of corresponding introns of *AG*- and *STK*-like genes, respectively, present in the NCBI public nucleotide database (Table 2) were analyzed to search for patterns of shared elements using the motif-based sequence analysis tool MEME [42]. These sequences were also scanned using the PLANTPAN database of plant transcription factor binding sites and *cis*-regulatory elements [43].

Results

The cDNA sequence of *OitaAG* (1,149 bp) includes a 5′- and 3′- UTR of 208 and 235 bp, respectively, and virtually

Table 1 Species, locus name and accession number of the sequences used to construct the ML tree

Order	Family	Species	Locus	Class	Accession number
Arecales	Arecaceae	*Elaeis guineensis*	*EguiAG1*	C	AY739698
			EguiAG2	C	AY739699
Asparagales	Agapanthaceae	*Agapanthus praecox*	*ApMADS2*	D	AB079260
	Alliaceae	*Allium cepa*	*AcepAG*	C	CF441435
	Amaryllidaceae	*Narcissus tazetta*	*NtazAG*	C	EF421828
	Asparagaceae	*Asparagus virgatus*	*AVAG1*	C	AB125347
			AVAG2	D	AB175825
		Hosta plantaginea	*HplaAG*	C	EU429307
	Hyacinthaceae	*Hyacintus orientalis*	*HAG1*	C	AF099937
			HoMADS1	D	AF194335
	Iridaceae	*Crocus sativus*	*CsatAG*	C	AY555580
	Orchidaceae	*Cymbidium ensifolium*	*CeMADS1*	C	GU123626
			CeMADS2	C	GU123627
		Dendrobium crumenatum	*DcOAG1*	C	DQ119840
			DcOAG2	D	DQ119841
		Dendrobium nobile	*DnobMADS2*		EF535599
		Dendrobium thyrsiflorum	*DthyrAG1*	C	DQ017702
			DthyrAG2	D	DQ017703
		Orchis italica	*OitaAG*	C	JX205496*
			OitaSTK	D	JX205497*
		Phalaenopsis equestris	*PeMADS1*	C	AF234617
			PeMADS7	D	JN983500
		Phalaenopsis hybrid cultivar	*PhalAG1*	C	AB232952
			PhalAG2	D	AB232953
Liliales	Liliaceae	*Lilium formosanum*	*LforAG*	C	HQ234917
		Lilium hybrid cultivar	*LLAG*	C	HM030993
		Lilium longiflorum	*LMADS2*	D	AY522502
			LLAG1	C	AY500376
			LLMADS1	C	AY829227
Pandanales	Triuridaceae	*Lacandonia schismatica*	*LschSTK*	D	GQ214164
Poales	Bromeliaceae	*Ananas comosus*	*AcomAG*	C	TA1404_4615
	Poaceae	*Hordeum vulgare*	*HvAG1*	C	AF486648
			HvAG2	C	AF486649
		Oryza sativa	*OsMADS13*	D	AF151693
			OsMADS58	C	AB232157
			OsMADS3	C	L37528
			OsMADS21	D	AY551913
		Sorghum bicolor	*SbicAG*	C	XM_002454940
		Triticum aestivum	*WAG*	C	AB084577
			TaAGL2	C	DQ512337
			TaAGL31	C	DQ512349
			TaAGL39	C	DQ512355
		Zea mays	*ZMM1*	C	X81199
			ZAG1	C	L18924
			ZAG2	C	L18925
			Zmay23	C	AJ430637
			Zmay3	C	EU960810
			ZmayAG	C	NM_001112476

Table 1 continued

Order	Family	Species	Locus	Class	Accession number
			ZMM2	C	AJ430631
			ZMM25	D	AJ430639
Zingiberales	Musaceae	*Musa acuminata*	*MacuMADS5*	D	DQ060444
	Zingiberaceae	*Alpinia hainanensis*	*AhaiAG*	C	AY621155
Coniferales	Pinaceae	*Picea abies*	*DAL2*	C	X79280

The asterisk indicates sequences obtained in the present study

Table 2 Species name, abbreviation, accession number and sequence size of the intron 2 (*AG*-like gene) and intron 1 (*STK*-like gene) examined

Species	Locus	Intron	Abbreviation	Accession number	Length (bp)
Orchis italica	*AG*-like	2	*OitaAG*	JX205498*	11,165
Antirrhinum majus			*PLE*	AY935269	6,666
Oryza sativa			*OsMADS3*	AP008207	5,351
Populus trichocarpa			*PTAG1*	AF052570	4,865
Petunia hybrida			*PMADS3*	AB076051	4,010
Ipomea nil			*DP*	AB281192	3,432
Solanum lycopersicum			*TAG1*	AY254705	3,190
Arabidopsis thaliana			*AG*	At4g18960	2,999
Antirrhinum majus			*FAR*	AJ239057	2,965
Cucumis sativus			*CUM1*	AY254704	1,903
Oryza sativa	*STK*-like	1	*OsMADS13*	Os12g10540	1,362
Arabidopsis thaliana			*STK*	AT4G09960	1,328
Zea mays			*ZAG2*	NM_001111908	1,261
Orchis italica			*OitaSTK*	JX205499*	97

The asterisk indicates sequences obtained in the present study

encodes for a protein of 234 residues. BLASTN and TBLASTX analyses revealed that the sequence with the highest similarity to *OitaAG* cDNA was the *AG1* sequence of the orchid *D. crumenatum* (88 % nucleotide and 87 % amino acid identity). The cDNA sequence of *OitaSTK* (903 bp) includes a 5′- and 3′- UTR of 105 and 113 bp, respectively, and virtually encodes for a protein of 227 residues. BLASTN and TBLASTX analyses of *OitaSTK* cDNA showed the highest similarity with the *AG2* sequence of the orchid *D. crumenatum* (82 % nucleotide and 84 % amino acid identity).

Amino acid alignment of virtually translated *OitaAG* and *OitaSTK* cDNA sequences with AG-like and STK-like monocot sequences present in GenBank revealed the presence of the two conserved regions in the C-terminus, the AG motifs I and II. The OitaAG sequence has an additional short amino acid stretch (7 residues) at the N-terminus, a feature common to many AG-like proteins. The OitaSTK sequence shows an extension of 6 amino acid residues at the C-terminus, known as the MD motif, common to the D-class proteins of monocots [44]. Figure 1 shows the amino acid alignment and the conserved motifs relative to the orchid sequences.

The ML tree was constructed using the JTT + G + I amino acid evolutionary model, and the bootstrap consensus tree is shown in Fig. 2. The tree topology shows two main branches corresponding to the MADS-box functional classes C and D. OitaAG forms a statistically well-supported group with the other orchid AG-like sequences within the C-class clade (bootstrap value 86 %), whereas OitaSTK is included within the D-class clade.

Figure 3c and d shows the expression profile of the *OitaAG* and *OitaSTK* genes in early and late floral tissues (Fig. 3b). The expression of mRNA from both genes is detectable mainly in the column, with a significant difference in the expression of *OitaSTK* between early and late stage tissues. Weak expression of *OitaAG* is detectable in late inner tepals, and a low level of *OitaSTK* mRNA is present in late lip tissue. The *OitaAG* and *OitaSTK* genes are also expressed in the ovary before pollination, where the level of *OitaSTK* transcripts is much higher than that of *OitaAG* (Fig. 4a). The expression of both genes begins to increase 3 days after pollination (3 dap); the highest levels are observed at the stages 7 and 10 dap. The expression of *OitaSTK* mRNA is much higher than that of *OitaAG* in both

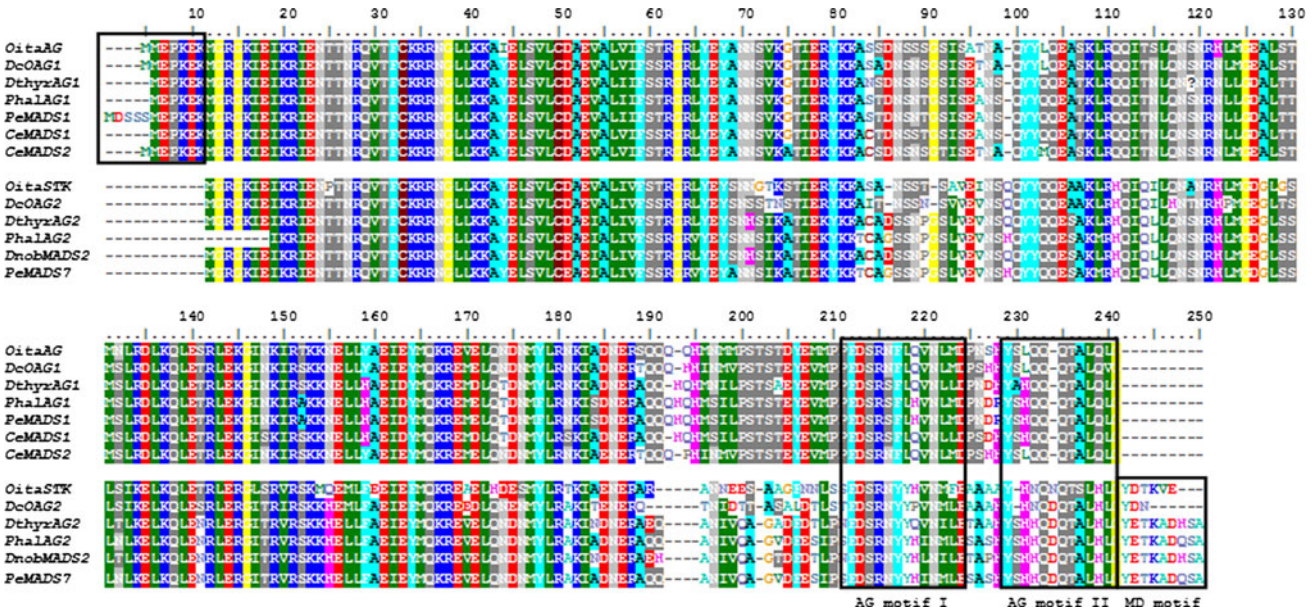

Fig. 1 Amino acid alignment of the *OitaAG* and *OitaSTK* sequences to those of the other orchid species. *Boxes* indicate the N-terminal extension, the *AG motif I* and *II* and the *MD motif*

pollinated and unpollinated ovaries (Fig. 4a). The expression level of *OitaAG* in root and stem tissue is comparable to that in the reference tissue (leaf), whereas a slightly higher level of *OitaSTK* mRNA is detectable in root tissue (Fig. 4b).

The genomic structure of the *OitaAG* and *OitaSTK* loci is presented in Fig. 5. *OitaAG* includes eight introns, and *OitaSTK* has seven; all the sequenced introns contain 5′-GT and 3′-AG termini. Intron 1 is located within the 5′-UTR in both genes, whereas intron 8 of the *OitaAG* locus is located within the codon preceding the TAG stop codon. As shown in Fig. 5, intron size is quite variable, whereas intron position is conserved, resulting in a similar exon size. The very large intron 3 of the *OitaAG* gene was amplified but not sequenced. All of the attempts to amplify intron 2 of the *OitaSTK* gene gave negative results. The CENSOR analysis revealed traces of transposable elements belonging to different classes present mainly within the largest introns (Table 3), though some short sequences similar to transposable elements were found within the small introns 4 and 8 of the *OitaAG* gene. Among the 25 traces of repetitive/mobile elements identified, 17 shared homology to Class I retrotransposons (9 LTR Copia or Gypsy and 8 NonLTR), 6 to Class II DNA transposons (4 En/Spm, 1 Helitron and 1 Mutator) and 2 to Interspersed repeats. The CENSOR analysis also highlighted traces of transposable elements within the nucleotide sequence of intron 2 of the *AG*-like genes retrieved from GenBank (Table S3, supplementary material), with a lower density relative to intron 2 of the *OitaAG* gene.

Intron 1 of the *OitaSTK* gene is considerably shorter than those of the other *STK*-like genes here examined (Table 2) and their nucleotide sequences are not alignable. MEME analysis revealed the presence of a single GA-rich motif (GAAGAAA) within intron 1 of the *OitaSTK* gene. In the corresponding region of the other *STK*-like genes MEME analysis identified 5 (*STK* and *OsMADS13*) and 7 (*ZAG2*) GA-rich motifs. In all of the examined sequences, PLANTPAN analysis showed the presence of a number of known transcription factor binding sites (TFBSs) (Table S4, supplementary material).

Introns 2 and 3 of the *OitaAG* gene are very large (11,165 and ∼15,000 bp, respectively), and to date, these are the largest introns 2 and 3 of the known *AG*-like genes. The nucleotide sequence of intron 2 of the *OitaAG* gene is not alignable to those of the other *AG*-like genes here examined due to their global sequence divergence. However, MEME analysis revealed the presence of conserved boxes corresponding to previously known *cis*-acting *AG* regulatory motifs within intron 2 of the *OitaAG* gene [27, 30]: the aAGAAT-box, the LEAFY binding site (LBS) and the 70 bp element known as CCAATCA-box are present in conserved order and conserved distance relative to the other examined sequences (Fig. 6). PLANTPAN analysis revealed the presence of a number of known TFBSs in all of the examined sequences (Table S4, supplementary material). Binding sites of WUSCHEL (WUS) and BELLRINGER (BLR) are present in *OitaAG* and in almost all of the other sequences. WUS and BLR are known as positive and negative regulators of *AG*, respectively [45, 46]. Furthermore, an AP2 binding site recently characterized in intron 2 of the *AG* gene of *A. thaliana* [28] was found within intron 2 of the *OitaAG* locus

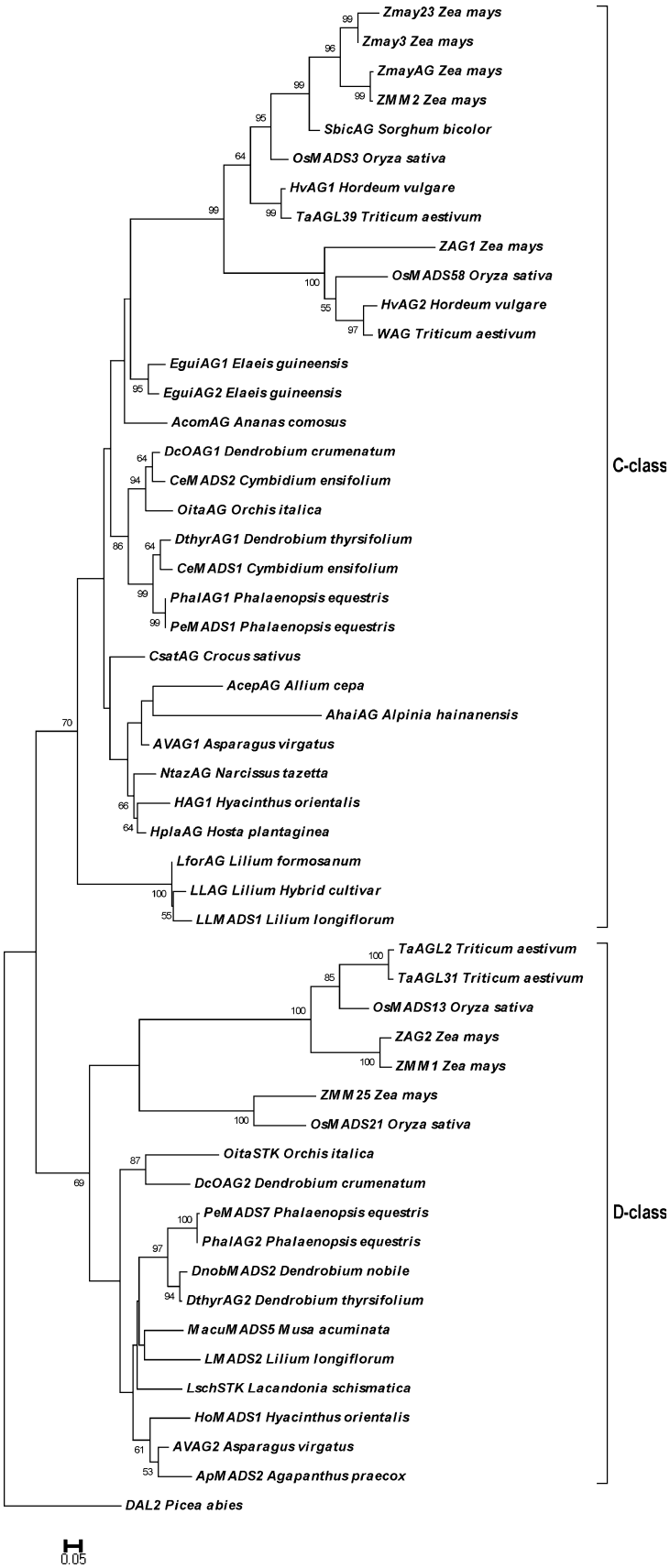

Fig. 2 Maximum Likelihood tree constructed on the amino acid alignment of the sequences listed in Table 1. *Numbers* indicate the bootstrap percentages (values lower than 50 % are not shown)

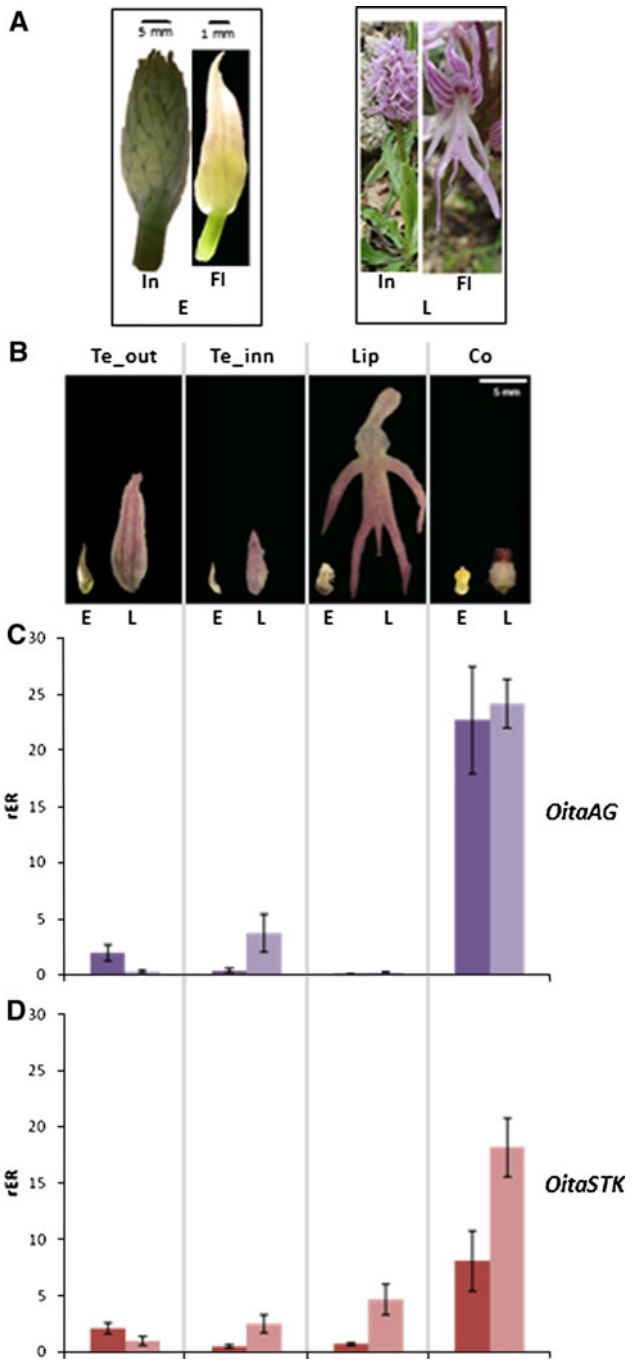

Fig. 3 Early (*left*) and late (*right*) inflorescence and floret of *O. italica* (**a**). Early (*left*) and late (*right*) floral tissue of *O. italica* (**b**) and the relative expression pattern of the *OitaAG* (**c**) and *OitaSTK* (**d**) genes: *In* inflorescence, *Fl* floret, *E* early, *L* late, *Te_out* outer tepal, *Te_inn* inner tepal, *Lip* labellum, *Co* column, *rER* relative expression ratio

downstream of the CCAATCA-box. In most of the intron 2 sequences examined in *OitaAG* and other genes, the size of the region between the CCAATCA-box and the AP2 binding site is quite variable (Fig. 6).

Discussion

In orchids, the column contains fused male and female tissues and ovule development is triggered by pollination. These peculiar reproductive structures are of particular interest when studying the role of the C- and D-class MADS-box genes in orchids.

Nucleotide/amino acid sequence comparison and phylogenetic analysis revealed that the *OitaAG* and *OitaSTK* genes of *O. italica* (Orchidoideae) belong to the C- and D-class MADS-box genes, respectively, and that these genes are closely related to the *AG*-like and *STK*-like genes isolated in Epidendroideae.

Like other *AG*-like genes, e.g. *ZAG1* of maize [47], *TAG1* of tomato [48], *AVAG1* of *Asparagus* [49], etc., *OitaAG* is specifically expressed in floral tissues. Similarly to other *STK*-like genes, e.g. *FBP11* of *Petunia* [50], *LMADS2* of lily [51], *AVAG2* of *Asparagus* [44], also *OitaSTK* is expressed in floral tissues. However, an unexpected weak expression of *OitaSTK* is detectable also in roots. Based on functional studies available in literature, C- and D-class MADS-box genes are not expressed in roots; instead, the sister C/D-class gene *XAL1* (*AGL12* group) is root-specific in *Arabidopsis* [52, 53] and rice [54]. Further studies are needed to understand if the weak expression of the *OitaSTK* gene detected in root tissue reflects its involvement in root development of *O. italica* or represents its background expression level in this tissue.

The *OitaAG* and *OitaSTK* genes display a similar expression pattern that confirms their involvement in the development and maintenance of reproductive structures, as is expected for these functional classes of MADS-box genes. Although the general similarity in the expression profiles of *OitaAG* and *OitaSTK* indicates a possible redundant function, some differences are detectable. In particular, *OitaAG* is expressed at similar levels in early and late column tissue, whereas the amount of the *OitaSTK* mRNA increases from early to late stages. This difference suggests a not completely redundant role for these two genes during the cell distension of gynostemium in *O. italica*, with *OitaAG* involved both in the formation and maintenance of the column and *OitaSTK* implicated mainly in the maintenance of this structure. In the ovary, the expression level of *OitaAG* is very low before fertilization and starts to increase at the 3 dap stage, reaching the highest level at the 7 and 10 dap stage. *OitaSTK* mRNA is strongly expressed in the unpollinated ovary, and fertilization further enhances its accumulation at the 3 dap stage and, more strongly, at 7 and 10 dap. This difference in expression profiles suggests a relevant role of the *OitaSTK* gene in ovary formation and maturation, while the C-class gene *OitaAG* seems to be involved only in events subsequent to pollination. This expression profile is only partially overlapping with that described in *Phalaenopsis*, where the *PeMADS1*

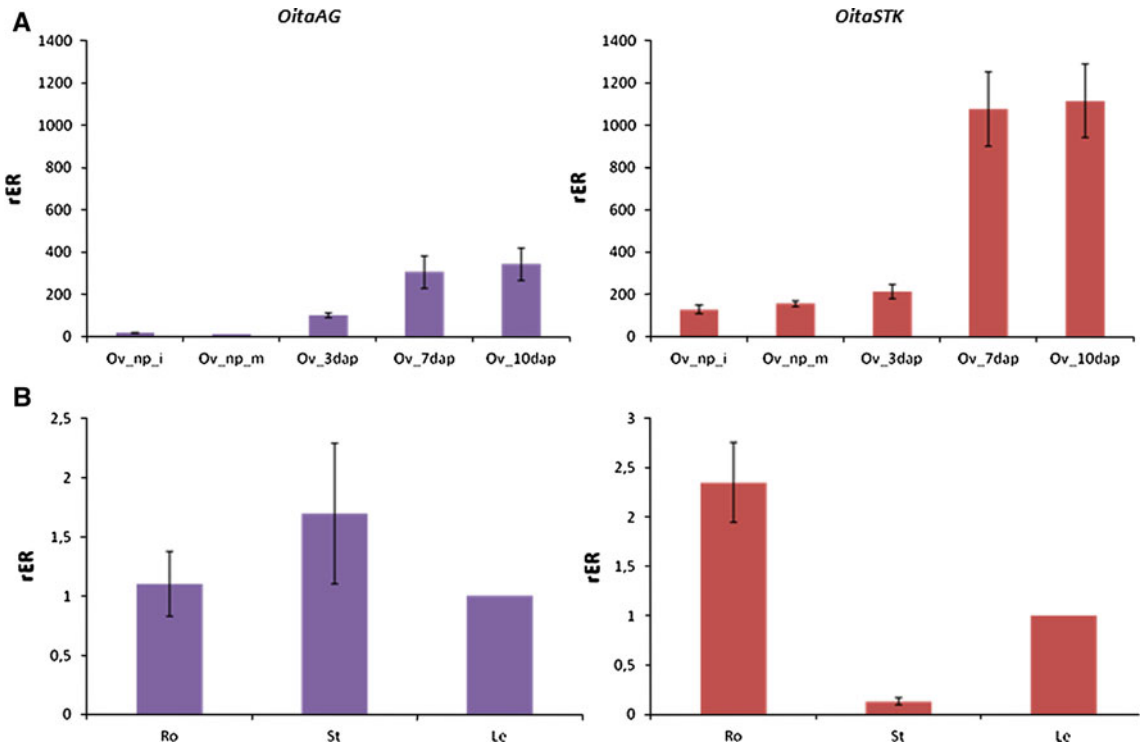

Fig. 4 Relative expression analysis of *OitaAG* and *OitaSTK* in the ovary (**a**) and non-floral tissues (**b**): *Ov_np_i* early ovary not pollinated, *Ov_np_m* late ovary not pollinated, *dap* days after pollination, *Ro* root, *St* stem, *Le* leaf, *rER* relative expression ratio

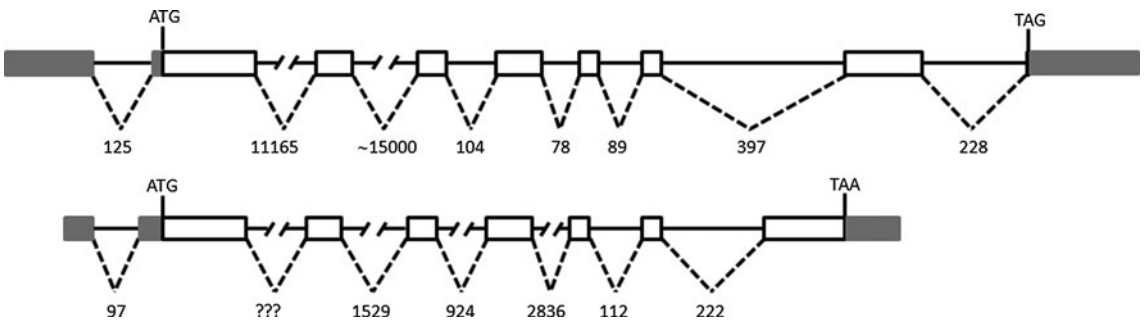

Fig. 5 Schematic diagram of the *OitaAG* (*upper*) and *OitaSTK* (*lower*) loci. *Gray boxes*, *white boxes* and *lines* indicate UTRs, exons and introns, respectively. *Numbers* represent the intron size in bp. Diagrams are in scale, with the exception of the *interrupted lines*. *ATG start codon* and *stop codons* are also indicated. *Question marks* indicate unknown size of the intron

(C-class) and *PeMADS7* (D-class) genes are both expressed at very low levels in the immature ovary, with expression increasing only after pollination [25]. In addition, other discrepancies are detectable when comparing the expression profile of the *OitaAG* and *OitaSTK* genes of *O. italica* to that of their homologs in other orchid species, especially within tepal, lip and vegetative tissue. *OitaAG* shows a weak expression in the inner tepal at the late stage, and *OitaSTK* mRNA is present at low levels in late stage lip tissue and in root tissue. Previous studies report the expression of the *DcOAG1* gene (C-class) of *D. crumenatum* and of the *PhalAG1* (C-class) and *PhalAG2* (D-class) genes of *Phalaenopsis* in tepals and lip tissue [22, 55]. In recent experiments, however, the expression of the *PeMADS1* and *PeMADS7* genes of *Phalaenopsis* was detected only in the column and post-pollinated ovary [25]. These contrasting results might be the result of different evolutionary histories of C-and D-class genes in orchids, a hypothesis also supported by the finding of two C-class genes with distinct roles during gynostemium development in *C. ensifolium* [24].

The presence of *cis*-regulatory elements within intron 2 of *AG*-like genes and intron 1 of *STK*-like genes has been evaluated mainly in dicots species, whereas in monocots, analyses have been restricted to rice. For this reason, we decided to determine the position and sequence of introns in both the *OitaAG* and *OitaSTK* genes of *O. italica*. The

Table 3 Results of the CENSOR analysis conducted on the introns of *OitaAG* and *OitaSTK*

Gene	Intron	Length (bp)	From	To	Element	From	To	Class	Dir	Sim	E-value
OitaAG	2	11,165	1,029	1,218	ENSPM-6_ZM	6,760	6,932	DNA/EnSpm	d	0.69	3e−08
			1,890	1,968	DNA9-3C_Mad	226	301	Interspersed_Repeat	c	0.78	1e−06
			4,557	4,619	MuDR1_HV	526	591	DNA/MuDR	c	0.72	0.004
			6,715	6,876	ATCOPIA70_I	4,321	4,482	LTR/Copia	c	0.69	1e−07
			7,158	7,630	Copia-2_PD-I	1,636	2,126	LTR/Copia	c	0.70	9e−45
			8,237	8,401	ENSPM-6_ZM	5,762	5,914	DNA/EnSpm	d	0.70	2e−06
			8,561	8,695	RTE-1_Mad	8,202	8,335	NonLTR/RTE	c	0.69	8e−05
			8,738	8,854	RTE-1_Mad	2,956	3,072	NonLTR/RTE	c	0.67	8e−05
			8,868	9,965	RTE-1B_Mad	1,744	2,851	NonLTR/RTE	c	0.64	2e−30
			10,733	10,802	EnSpm-12_OS	10,612	10,680	DNA/EnSpm	c	0.76	0.003
	4	104	45	81	ATHILA-4_SBi-I	4,787	4,823	LTR/Gypsy	c	0.84	9e−06
	8	228	61	124	EnSpm-5_STu	8,852	8,917	DNA/EnSpm	c	0.78	2e−07
OitaSTK	3	1,529	545	620	RTE-1_Mad	8,267	8,342	NonLTR/RTE	c	0.78	1e−09
			664	748	Copia-55_BRa-I	2,201	2,281	LTR/Copia	d	0.75	6e−06
			1,080	1,133	Copia-100_Mad-I	40	90	LTR/Copia	c	0.81	3e−06
	4	924	213	379	SINE2-2_STu	1	165	NonLTR/SINE/SINE2	d	0.78	4e−28
			394	467	SINE2-2_STu	68	134	NonLTR/SINE/SINE2	d	0.78	6e−09
			509	562	SINE2-2_STu	66	120	NonLTR/SINE/SINE2	d	0.82	6e−09
			616	734	SINE2-2_STu	65	181	NonLTR/SINE/SINE2	d	0.80	1e−23
	5	2,836	381	486	HELITRON7_OS	1,567	1,679	DNA/Helitron	c	0.85	3e−22
			489	518	Gypsy-76_SB-I	2,574	2,603	LTR/Gypsy	d	0.90	9e−05
			794	828	DNA9-3C_Mad	528	562	Interspersed_Repeat	c	0.83	4e−05
			975	1,084	Copia1A-VV_I	4,422	4,533	LTR/Copia	c	0.73	5e−07
			1,110	1,914	Copia-8_CP-I	3,714	4,563	LTR/Copia	c	0.66	3e−04
			1,948	2,209	Copia2-VV_I	3,179	3,450	LTR/Copia	c	0.70	3e−17

Only introns showing positive matches are shown

Dir direction (*d* direct, *c* complement), *Sim* nucleotide similarity, *E-value* the BLAST expectation value

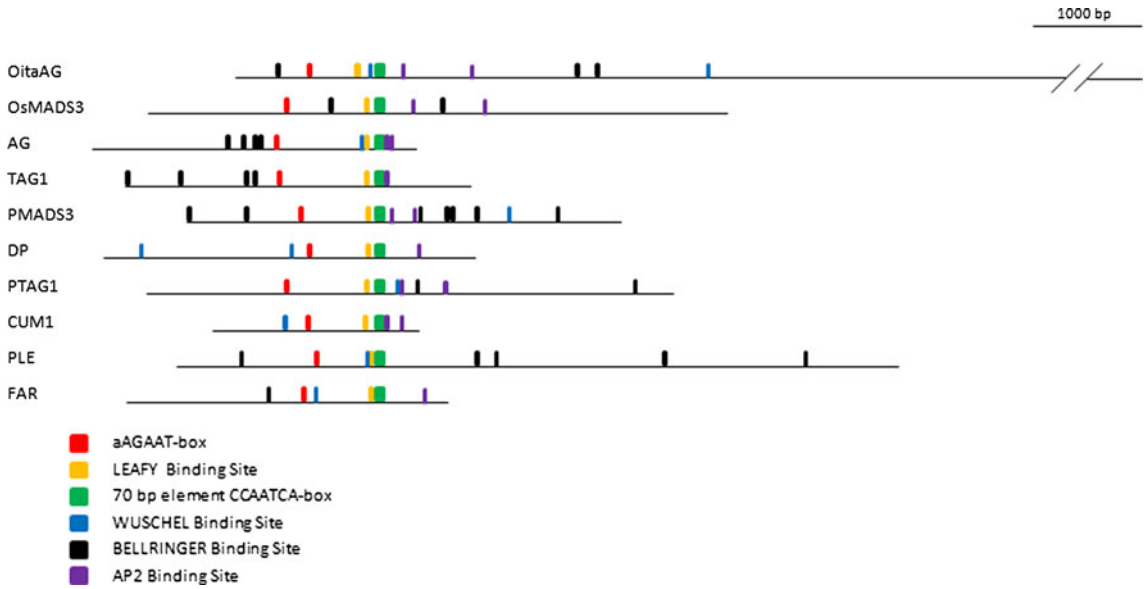

Fig. 6 Schematic diagram showing the *conserved boxes* and TFBSs found within the nucleotide sequence of intron 2 of *OitaAG* and its homologs

common features of the sequenced introns are their conserved position relative to the exons and the frequent presence of traces of mobile elements within their sequence. The classification and relative abundance of these repetitive/mobile elements are similar, in a much smaller scale, to those reported in a partial genome analysis conducted on the orchid *Phalaenopsis* [56]. In particular, in both species Class I retrotransposons are highly represented (68 % in *O. italica* and 75.7 % in *Phalaenopsis*) and among them the most abundant are copia- and gypsy-like elements (36 % in *O. italica* and 54.7 % in *Phalaenopsis*). Class II transposons are less frequent than Class I retrotransposons (24 % in *O. italica* and 10.8 % in *Phalaenopsis*) and among them the most abundant are En/Spm elements (16 % in *O. italica* and 5.3 % in *Phalaenopsis*). The other identified repetitive/mobile elements (e.g. interspersed repeats, centromere, unclassified elements) represent 8 % in *O. italica* and 13.5 % in *Phalaenopsis*. The size of some of the isolated introns is quite small, in agreement with the general small size of introns in plant MIKC MADS-box genes. In contrast, the size of intron 2 of the *OitaAG* gene is very large and, to date, is the largest ever reported (11,165 bp). Also intron 3 of the *OitaAG* gene is very large (~15,000 bp) and the introns 3, 4 and 5 of the *OitaSTK* gene are quite large in size, although in a much smaller range (from 924 to 2,836 bp). It is possible that the insertion of mobile elements has contributed to the expansion of these noncoding regions. For example, a quite large (~850 bp) trace of an LTR/copia element is still detectable within intron 5 of the *OitaSTK* gene. In addition, BLAST analyses revealed that intron 2 of the *OitaAG* gene contains two regions (spanning from the position 2,900–3,099 and from 4,986 to 5,065) that show identity (~76 %) with two regions (the first inverted and the second direct) in intron 1 of the *LFY* gene of the orchid *Ophrys*. A similar result was obtained from a BLAST analysis with intron 2 from the *AG*-like gene *PMADS3* in *Petunia* that shows identity (~74 %) from position 3,487 to 3,635 with an inverted region of intron 2 of the *LFY* gene in *Capsicum lycianthoides*. This evidence indicates high and possibly recent activity of mobile elements that could also have captured genomic segments surrounding their original position and, after the insertion within the introns of the *OitaAG* and *OitaSTK* genes, undergone mutations and fragmentation leading to their inactivation.

Sequence comparison of intron 1 of the *STK*-like genes here examined revealed the presence of a single GA-rich motif within intron 1 of the *OitaSTK* gene. Even though GA-rich motifs were found by MEME analysis within intron 1 of the *OsMADS13* and *ZAG2* genes, their sequence does not exactly matches to that of the consensus motif RGARAGRRA that, present in multiple copies within intron 1 of the *STK* gene of *Arabidopsis*, in vitro binds the BPC1 protein. The absence of conservation of these *cis*-regulatory motifs within intron 1 of the *OitaSTK*, *OsMADS13* and *ZAG2* genes might indicate the existence of proteins different from BPC1 involved in the transcriptional regulation of D-class genes in monocots. Alternatively, in monocots all the BPC1 binding sites might be located in different positions, e.g. within the promoter, or have a different consensus sequence.

The most interesting feature of intron 2 of the *OitaAG* gene is the presence of conserved regulatory boxes functionally characterized in *A. thaliana*. The direct interaction of the LFY transcription factor with intron 2 of the *AG* gene in *Arabidopsis* is crucial for the early activation of *AG* expression [57]. The 70 bp element is involved in the late stage activity of AG [27], while the function of the aAGAAT-box is still not clear. These motifs (aAGAAT-box, LBS and the 70 bp element) were clearly identified by MEME analysis to be within the nucleotide sequence of intron 2 of *OitaAG*, with the same order and a similar relative distance as in the *Arabidopsis* gene. These features highlight the importance of the nucleotide sequence and spatial distribution conservation of the three *cis*-regulatory motifs in monocots as well as dicots. In addition to these three conserved motifs, the PLANTPAN search identified a number of putative TFBSs shared by intron 2 of the *OitaAG* gene and its homologs. Of particular interest is the presence of binding sites for known regulators of *AG*: WUS (positive regulator) and BLR (negative regulator). Both TFBSs are present in multiple copies within intron 2 of *OitaAG* and many of its homologs. The spatial location of these elements is not strictly conserved, particularly in monocots (orchid and rice). The absence of canonical WUS binding sites within intron 2 of the *OsMADS3* gene might be due to the partition of the C-class functions between *OsMADS3* and its paralogous gene *OsMADS58* in rice (sub-functionalization) [58, 59] and/or to the expression pattern of the *WUS* gene of rice (*OsWUS*), different from that of the *WUS* gene of *Arabidopsis* [60]. Finally, the *AG* gene is known to be negatively regulated by the A-class factor AP2 through direct interaction with a non-canonical AT-rich sequence located within intron 2 [28]. In some of the examined genes, the position of the AP2 binding sites in intron 2 is just downstream of the 70 bp element, whereas in *O. italica* and rice, it is farther downstream. The presence of conserved regions and TFBSs within intron 2 of the *OitaAG* gene of *O. italica* suggests that the general regulatory mechanisms of this gene are strictly conserved; however, differences in the number and distribution of the TFBSs might be related to peculiar aspects of the expression profile of this gene in orchids.

Acknowledgments The authors wish to thank Prof. Salvatore Cozzolino for supplying the plant material and performing the manual pollination of ovaries in *O. italica* and Dr. Maria Rosaria Barone Lumaga for the description of the ovary development stages. The authors are also grateful to Mrs. Rosaria Terracciano and Mr.

Vincenzo Iacueo for their technical support. This work was supported by the 2009 Regione Campania Grant L.R. N5/2002.

References

1. Yu H, Goh CJ (2001) Molecular genetics of reproductive biology in orchids. Plant Physiol 127(4):1390–1393
2. Tsai WC, Chen HH (2006) The orchid MADS-box genes controlling floral morphogenesis. Sci World J 6:1933–1944
3. Rudall PJ, Bateman RM (2002) Roles of synorganisation, zygomorphy and heterotopy in floral evolution: the gynostemium and labellum of orchids and other lilioid monocots. Biol Rev Camb Philos Soc 77(3):403–441
4. Coen ES, Meyerowitz EM (1991) The war of the whorls—genetic interactions controlling flower development. Nature 353(6339):31–37
5. Krizek BA, Fletcher JC (2005) Molecular mechanisms of flower development: an armchair guide. Nat Rev Genet 6(9):688–698
6. Causier B, Schwarz-Sommer Z, Davies B (2010) Floral organ identity: 20 years of ABCs. Semin Cell Dev Biol 21(1):73–79
7. Ambrose BA, Lerner DR, Ciceri P, Padilla CM, Yanofsky MF, Schmidt RJ (2000) Molecular and genetic analyses of the silky1 gene reveal conservation in floral organ specification between eudicots and monocots. Mol Cell 5(3):569–579
8. Whipple CJ, Ciceri P, Padilla CM, Ambrose BA, Bandong SL, Schmidt RJ (2004) Conservation of B-class floral homeotic gene function between maize and *Arabidopsis*. Development 131(24): 6083–6091
9. Whipple CJ, Zanis MJ, Kellogg EA, Schmidt RJ (2007) Conservation of B class gene expression in the second whorl of a basal grass and outgroups links the origin of lodicules and petals. Proc Natl Acad Sci USA 104(3):1081–1086
10. Kim S, Koh J, Yoo MJ, Kong H, Hu Y, Ma H, Soltis PS, Soltis DE (2005) Expression of floral MADS-box genes in basal angiosperms: implications for the evolution of floral regulators. Plant J 43(5):724–744
11. Ferrario S, Immink RG, Angenent GC (2004) Conservation and diversity in flower land. Curr Opin Plant Biol 7(1):84–91
12. Aceto S, Gaudio L (2011) The MADS and the beauty: genes involved in the development of orchid flowers. Curr Genomics 12(5):342–356
13. Mondragon-Palomino M, Theissen G (2011) Conserved differential expression of paralogous DEFICIENS- and GLOBOSA-like MADS-box genes in the flowers of Orchidaceae: refining the 'orchid code'. Plant J 66(6):1008–1019
14. Cantone C, Sica M, Gaudio L, Aceto S (2009) The OrcPI locus: genomic organization, expression pattern, and noncoding regions variability in *Orchis italica* (Orchidaceae) and related species. Gene 434(1–2):9–15
15. Cantone C, Gaudio L, Aceto S (2011) The GLO-like locus in orchids: duplication and purifying selection at synonymous sites within Orchidinae (Orchidaceae). Gene 481:48–55
16. Salemme M, Sica M, Gaudio L, Aceto S (2011) Expression pattern of two paralogs of the PI/GLO-like locus during *Orchis italica* (Orchidaceae, Orchidinae) flower development. Dev Genes Evol 221(4):241–246
17. Aceto S, Montieri S, Sica M, Gaudio L (2007) Molecular evolution of the OrcPI locus in natural populations of Mediterranean orchids. Gene 392(1–2):299–305
18. Tsai WC, Kuoh CS, Chuang MH, Chen WH, Chen HH (2004) Four DEF-like MADS box genes displayed distinct floral morphogenetic roles in *Phalaenopsis* orchid. Plant Cell Physiol 45(7): 831–844
19. Tsai WC, Lee PF, Chen HI, Hsiao YY, Wei WJ, Pan ZJ, Chuang MH, Kuoh CS, Chen WH, Chen HH (2005) PeMADS6, a GLOBOSA/PISTILLATA-like gene in *Phalaenopsis equestris* involved in petaloid formation, and correlated with flower longevity and ovary development. Plant Cell Physiol 46(7): 1125–1139
20. Pan ZJ, Cheng CC, Tsai WC, Chung MC, Chen WH, Hu JM, Chen HH (2011) The duplicated B-class MADS-box genes display dualistic characters in orchid floral organ identity and growth. Plant Cell Physiol 52(9):1515–1531
21. Hsu HF, Hsieh WP, Chen MK, Chang YY, Yang CH (2010) C/D class MADS box genes from two monocots, orchid (*Oncidium Gower Ramsey*) and lily (*Lilium longiflorum*), exhibit different effects on floral transition and formation in *Arabidopsis thaliana*. Plant Cell Physiol 51(6):1029–1045
22. Song IJ, Nakamura T, Fukuda T, Yokoyama J, Ito T, Ichikawa H, Horikawa Y, Kameya T, Kanno A (2006) Spatiotemporal expression of duplicate AGAMOUS orthologues during floral development in *Phalaenopsis*. Dev Genes Evol 216(6):301–313
23. Skipper M, Johansen LB, Pedersen KB, Frederiksen S, Johansen BB (2006) Cloning and transcription analysis of an AGAMOUS- and SEEDSTICK ortholog in the orchid *Dendrobium thyrsiflorum* (Reichb. f.). Gene 366(2):266–274
24. Wang SY, Lee PF, Lee YI, Hsiao YY, Chen YY, Pan ZJ, Liu ZJ, Tsai WC (2011) Duplicated C-class MADS-box genes reveal distinct roles in gynostemium development in *Cymbidium ensifolium* (Orchidaceae). Plant Cell Physiol 52(3):563–577
25. Chen YY, Lee PF, Hsiao YY, Wu WL, Pan ZJ, Lee YI, Liu KW, Chen LJ, Liu ZJ, Tsai WC (2012) C- and D-class MADS-box genes from *Phalaenopsis equestris* (Orchidaceae) display functions in gynostemium and ovule development. Plant Cell Physiol 53(6):1053–1067
26. Kramer EM, Jaramillo MA, Di Stilio VS (2004) Patterns of gene duplication and functional evolution during the diversification of the AGAMOUS subfamily of MADS box genes in angiosperms. Genetics 166(2):1011–1023
27. Hong RL, Hamaguchi L, Busch MA, Weigel D (2003) Regulatory elements of the floral homeotic gene AGAMOUS identified by phylogenetic footprinting and shadowing. Plant Cell 15(6): 1296–1309
28. Dinh TT, Girke T, Liu X, Yant L, Schmid M, Chen X (2012) The floral homeotic protein APETALA2 recognizes and acts through an AT-rich sequence element. Development 139(11):1978–1986
29. Deyholos MK, Sieburth LE (2000) Separable whorl-specific expression and negative regulation by enhancer elements within the AGAMOUS second intron. Plant Cell 12(10):1799–1810
30. Causier B, Bradley D, Cook H, Davies B (2009) Conserved intragenic elements were critical for the evolution of the floral C-function. Plant J 58(1):41–52
31. Kooiker M, Airoldi CA, Losa A, Manzotti PS, Finzi L, Kater MM, Colombo L (2005) BASIC PENTACYSTEINE1, a GA binding protein that induces conformational changes in the regulatory region of the homeotic arabidopsis gene SEEDSTICK. Plant Cell 17(3):722–729
32. Zhao S, Fernald RD (2005) Comprehensive algorithm for quantitative real-time polymerase chain reaction. J Comput Biol 12(8):1047–1064
33. Schefe JH, Lehmann KE, Buschmann IR, Unger T, Funke-Kaiser H (2006) Quantitative real-time RT-PCR data analysis: current concepts and the novel "gene expression's CT difference" formula. J Mol Med 84(11):901–910
34. Doyle JJ, Doyle JL (1987) A rapid DNA isolation procedure for small amounts of leaf tissue. Phytochem Bull 19:11–15
35. Montieri S, Gaudio L, Aceto S (2004) Isolation of the LFY/FLO homologue in *Orchis italica* and evolutionary analysis in some European orchids. Gene 333:101–109

36. Keeney S (2011) Long-PCR amplification of human genomic DNA. Methods Mol Biol 688:67–74
37. Edgar RC (2004) MUSCLE: multiple sequence alignment with high accuracy and high throughput. Nucleic Acids Res 32(5):1792–1797
38. Zahn LM, Leebens-Mack JH, Arrington JM, Hu Y, Landherr LL, dePamphilis CW, Becker A, Theissen G, Ma H (2006) Conservation and divergence in the AGAMOUS subfamily of MADS-box genes: evidence of independent sub- and neofunctionalization events. Evol Dev 8(1):30–45
39. Tamura K, Peterson D, Peterson N, Stecher G, Nei M, Kumar S (2011) MEGA5: molecular evolutionary genetics analysis using maximum likelihood, evolutionary distance, and maximum parsimony methods. Mol Biol Evol 28(10):2731–2739
40. Hall TA (1999) BioEdit: a user-friendly biological sequence alignment editor and analysis program for Windows 95/98/NT. Nucl Acids Symp Ser 41:95–98
41. Kohany O, Gentles AJ, Hankus L, Jurka J (2006) Annotation, submission and screening of repetitive elements in Repbase: repbaseSubmitter and censor. BMC Bioinformatics 7:474
42. Bailey TL, Boden M, Buske FA, Frith M, Grant CE, Clementi L, Ren J, Li WW, Noble WS (2009) MEME SUITE: tools for motif discovery and searching. Nucleic Acids Res 37 (Web Server issue):W202–W208
43. Chang WC, Lee TY, Huang HD, Huang HY, Pan RL (2008) PlantPAN: plant promoter analysis navigator, for identifying combinatorial cis-regulatory elements with distance constraint in plant gene groups. BMC Genomics 9(1):561
44. Yun PY, Kim SY, Ochiai T, Fukuda T, Ito T, Kanno A, Kameya T (2004) AVAG2 is a putative D-class gene from an ornamental asparagus. Sex Plant Reprod 17(3):107–116
45. Bao X, Franks RG, Levin JZ, Liu Z (2004) Repression of AGAMOUS by BELLRINGER in floral and inflorescence meristems. Plant Cell 16(6):1478–1489
46. Ikeda M, Mitsuda N, Ohme-Takagi M (2009) *Arabidopsis* WUSCHEL is a bifunctional transcription factor that acts as a repressor in stem cell regulation and as an activator in floral patterning. Plant Cell 21(11):3493–3505
47. Schmidt RJ, Veit B, Mandel MA, Mena M, Hake S, Yanofsky MF (1993) Identification and molecular characterization of ZAG1, the maize homolog of the *Arabidopsis* floral homeotic gene AGAMOUS. Plant Cell 5(7):729–737
48. Pnueli L, Hareven AD, Rounsley SD, Yanofsky MF, Lifschitz E (1994) Isolation of the tomato agamous gene *Tag1* and analysis of its homeotic role in transgenic plants. Plant Cell 6(2):163–173
49. Yun PY, Ito T, Kim SY, Kanno A, Kameya T (2004) The AVAG1 gene is involved in development of reproductive organs in the ornamental asparagus *Asparagus virgatus*. Sex Plant Reprod 17(1):1–8
50. Colombo L, Franken J, Koetje E, van Went J, Dons HJ, Angenent GC, van Tunen AJ (1995) The petunia MADS box gene FBP11 determines ovule identity. Plant Cell 7(11):1859–1868
51. Tzeng TY, Chen HY, Yang CH (2002) Ectopic expression of carpel-specific MADS box genes from lily and lisianthus causes similar homeotic conversion of sepal and petal in *Arabidopsis*. Plant Physiol 130(4):1827–1836
52. Rounsley SD, Ditta GS, Yanofsky MF (1995) Diverse roles for MADS box genes in *Arabidopsis* development. Plant Cell 7(8): 1259–1269
53. Tapia-Lopez R, Garcia-Ponce B, Dubrovsky JG, Garay-Arroyo A, Perez-Ruiz RV, Kim SH, Acevedo F, Pelaz S, Alvarez-Buylla ER (2008) An AGAMOUS-related MADS-box gene, XAL1 (AGL12), regulates root meristem cell proliferation and flowering transition in *Arabidopsis*. Plant Physiol 146(3):1182–1192
54. Lee S, Woo YM, Ryu SI, Shin YD, Kim WT, Park KY, Lee IJ, An G (2008) Further characterization of a rice AGL12 group MADS-box gene, OsMADS26. Plant Physiol 147(1):156–168
55. Xu Y, Teo LL, Zhou J, Kumar PP, Yu H (2006) Floral organ identity genes in the orchid *Dendrobium crumenatum*. Plant J 46(1): 54–68
56. Hsu CC, Chung YL, Chen TC, Lee YL, Kuo YT, Tsai WC, Hsiao YY, Chen YW, Wu WL, Chen HH (2011) An overview of the *Phalaenopsis* orchid genome through BAC end sequence analysis. BMC Plant Biol 11:3
57. Weigel D, Meyerowitz EM (1993) Activation of floral homeotic genes in *Arabidopsis*. Science 261(5129):1723–1726
58. Yamaguchi T, Lee DY, Miyao A, Hirochika H, An G, Hirano HY (2006) Functional diversification of the two C-class MADS box genes OSMADS3 and OSMADS58 in *Oryza sativa*. Plant Cell 18(1):15–28
59. Hu L, Liang W, Yin C, Cui X, Zong J, Wang X, Hu J, Zhang D (2011) Rice MADS3 regulates ROS homeostasis during late anther development. Plant Cell 23(2):515–533
60. Nardmann J, Werr W (2006) The shoot stem cell niche in angiosperms: expression patterns of WUS orthologues in rice and maize imply major modifications in the course of mono- and dicot evolution. Mol Biol Evol 23(12):2492–2504